Comprehensive screening of *CYP4V2* in a cohort of Chinese patients with Bietti crystalline dystrophy

Xiaohui Zhang,[1] Ke Xu,[1] Bing Dong,[1] Xiaoyan Peng,[1] Qian Li,[2] Feng Jiang,[1] Yue Xie,[1] Lu Tian,[1] Yang Li[1]

[1]*Beijing Institute of Ophthalmology, Beijing Tongren Eye Center, Beijing Tongren Hospital, Capital Medical University; Beijing Ophthalmology & Visual Sciences Key Laboratory, Beijing, China;* [2]*Department of Ophthalmology, Beijing Tongren Eye Center, Beijing Tongren Hospital, Capital Medical University; Beijing Ophthalmology & Visual Sciences Key Laboratory, Beijing, China*

Purpose: Bietti crystalline dystrophy (BCD) is an autosomal recessive retinal degeneration disorder caused by mutations in *CYP4V2*. The aim of this study is to describe the genetic and clinical findings in 128 unrelated Chinese patients diagnosed with BCD.
Methods: Ophthalmological evaluations were performed in all patients. All coding regions of *CYP4V2* were amplified and sequenced directly. Real-time quantitative PCR was performed to detect copy number variations. Haplotype analysis was performed in 70 patients with c.802−8_810del17insGC and in 93 normal controls.
Results: A total of 28 mutations in *CYP4V2*, including eight novel mutations, were identified in 125 patients. The most common mutation was c.802−8_810del17insGC, with an allele frequency of 62.6%, followed by p.H331P (8.7%) and c.1091−2A>G (7.5%). A novel large deletion encompassing exon 8 of *CYP4V2* was detected. Haplotype analysis revealed four common haplotypes in patients with c.802−8_810del17insGC. A 17.6 kb haplotype CT(delCT)TA(Indel)A was the most common and was observed in 34.5% of the c.802−8_810del17insGC mutant alleles. The patients with mutations in *CYP4V2* showed wide intra- and interfamilial variability in clinical severity.
Conclusions: The findings expand the mutational spectrum of *CYP4V2* and further confirm the c.802−8_810del17insGC mutation was due to a founder effect in a large cohort of Chinese patients.

Bietti crystalline dystrophy (OMIM 210370, BCD) is a specific kind of progressive retinal disorder [1]. This disorder is rare in Caucasian populations but is comparatively common in East Asia, particularly in China, where BCD occurs with an estimated gene frequency of 0.05 [2]. BCD is characterized by the presence of numerous yellow-white crystalline deposits at the posterior pole of the retina or the cornea, atrophy of the RPE, and choroidal sclerosis [1,3,4]. Patients usually experience nyctalopia, decreased visual acuity, and paracentral scotomas during their second to fourth decade of life [1,3]. Furthermore, a recent study showed that photoreceptors were relatively preserved in BCD [5], implying that BCD is a good adaptation disease of regenerative therapy. BCD is inherited in an autosomal recessive inheritance mode, and all patients carry mutations in *CYP4V2* [3-12].

The *CYP4V2* gene (Gene ID 285440, OMIM 210370) comprises 11 exons and encodes a protein of 525 amino acids. The CYP4V2 protein belongs to the cytochrome P450 family 4 and is expressed in almost all tissues but is highly expressed in the retina and the RPE and less expressed in the cornea [3,13]. Metabolic studies of lymphocytes and fibroblasts cultured from patients with BCD have shown abnormally high triglycerides and cholesterol storage, with reduced conversion of fatty acid precursors into n-3 polyunsaturated fatty acids (PUFAs) [14]. The peripheral venous blood of patients with BCD exhibits reduced Δ-9-desaturase activity and an abnormally low concentration of total monounsaturated fatty acids [15].

To date, more than 80 disease-causing mutations in *CYP4V2* have been reported in patients with BCD [3-12,16-25]. More than half of the mutations are missense mutations, while the remaining mutations include nonsense mutations, small insertions or deletions, splicing defects, and large deletions. Several common mutations are specific to geographic or ethnic backgrounds, such as mutation c.802−8_810del17insGC (p.V268_E329del) in East Asian patients, with an allele frequency of 17.2% to 83.3% [3,6,7,10-12,25], p.Met66Arg in patients of South Asian ancestry, with an allele frequency of 47% [20], and p.I111T in Lebanese [16], Italian [17], and German patients [23], with an allele frequency of 15% to 66.7%. All these common mutations are founder mutations [7,10,16,17,25]. The aim of this study is to describe the genetic and clinical features of 128 unrelated Chinese patients diagnosed with BCD and to further verify the founder effect of the most common mutation, c.802−8_810del17insGC.

Correspondence to: Yang Li, Beijing institute of Ophthalmology, Beijing Tongren Hospital, Hougou Lane 17, Chong Nei Street, Beijing, 100730, China; Phone: 8610-58265915; FAX: 8610-65288561 or 65130796; email: yanglibio@aliyun.com

METHODS

Patients: This retrospective study was approved by the Medical Ethics Committee of Beijing Tongren Hospital, and all investigations were performed in accordance with the principles of the Declaration of Helsinki. The study also adhered to the ARVO statement on human subjects. In total, 128 unrelated patients with a clinical diagnosis of BCD were recruited from the Genetics Laboratory of Beijing Institute of Ophthalmology, Beijing Tongren Hospital, from 2002 to 2017. Six patients (cases 028029, 028041, 028042, 028044, 028049, and 028051) were described in a previous report by our study group [8], and a detailed clinical presentation of nine patients (cases 028092, 028094, 028095, 028097, 028099, 028104, 028111, 028113, and 028122) was described by our colleagues [26]. All enrolled patients were either sporadic (n=92) or showed a recessive mode of inheritance (n=36). Written informed consent was obtained from all participants. Ophthalmological evaluations including the best-corrected visual acuity (BCVA), slit-lamp biomicroscopy, fundus examination, and color fundus photography were performed on all patients. Some patients also underwent spectral domain optical coherence tomography (SD-OCT; Spectralis HRA+OCT, Heidelberg Engineering, Heidelberg, Germany), fundus autofluorescence (FAF; Spectralis HRA+OCT, Heidelberg Engineering), and electroretinogram (ERG; RETI-PORT21, Roland Consult, Brandenburg, Germany) examinations. The clinical diagnosis of BCD was based on the presence of yellow-white crystalline deposits at the posterior pole of the retina, together with the symptoms of nyctalopia or decreased visual acuity.

Based on the appearance of the color fundus images that were taken during the patients' first visit to the clinic, 128 patients were graded into stage 1, 2, or 3, using the classification proposed by Yuzawa and colleagues [27]. Stage 1 is characterized by RPE atrophy with uniform tiny crystalline deposits in the macular areas. Stage 2 is categorized by RPE atrophy extending beyond the macular area; RPE atrophy and choriocapillaris atrophy appear distinct in the macular areas of these patients. Stage 3 is differentiated by crystalline deposits, which varies in number, shape, and size; atrophy of the RPE and choriocapillaris was observed over the entire fundus in all of these patients (Figure 1).

Mutation screening of CYP4V2: Genomic DNA of all patients and available family members was extracted from peripheral blood leukocytes, following the manufacturer's instructions for the genomic DNA extraction kit (Vigorous, Beijing, China). Exons 1 to 11 and the flanking exon-intron boundaries of *CYP4V2* were amplified via PCR for all patients using the primers and conditions described previously [8]. The purified

PCR amplified products were sequenced with an ABI PRISM 3730 DNA sequencer (Applied Biosystems, Foster City, CA). Sequencing data were compared with the GenBank sequence for *CYP4V2* (accession number, NM_207352.3). The potential functional impacts of missense mutations were evaluated with Polymorphism Phenotyping 2 (Polyphen-2), Mutation Taster, Sorting Intolerant from Tolerant (SIFT), PMut, and GERP++. Splice site changes were analyzed with NetGene2. The variants were classified into pathogenic, likely pathogenic, variant of uncertain significance, likely benign, or benign according to the American College of Medical Genetics and Genomics (ACMG) standards and guidelines [28]. Allele-specific PCR was performed in the available family members and in 100 healthy controls to verify the variations identified in the sequencing. The allele frequency of the c.802–8_810del17insGC mutation was investigated with PCR-based sequencing in 421 normal controls.

Real-time quantitative PCR: To investigate the possible presence of large deletions in *CYP4V2*, real-time quantitative PCR was performed in patients 019122, 028141, and 028144. Real-time quantitative PCR was performed on a Rotor-Gene 6000 (Corbett Research, Mortlake, Australia). The reaction volume of 10 µl included 300 nM primers, 100 ng genomic DNA, and 2X SsoFast PCR Master Mix (Bio-Rad Laboratories, Hercules, CA). The primer sequences are shown in Table 1. After an initial denaturation at 98 °C for 2 min, reaction mixes underwent 40 cycles of 98 °C for 10 s, 60 °C for 10 s, and 72 °C for 10 s followed by 72 °C for 10 min. Each sample was replicated three times. The relative quantitation (RQ) of the target exon was performed using the 2-delta delta cycle threshold (2-ddCt) method [29]. All samples were normalized using glyceraldehyde-3-phosphate dehydrogenase (*GAPDH*) as an internal reference gene.

SNaPshot reaction and haplotype analysis: Genotypes of six intragenic single nucleotide polymorphisms (SNPs) flanking the c.802–8_810del17insGC mutation were analyzed in 93 unrelated healthy Chinese subjects, 70 patients carrying homozygous (n=40) or heterozygous (n=30) mutations, and any available relatives of these patients. These SNPs are located in the 5′-untranslated region (UTR), International Valuation Standard 2 (IVS2), IVS3, and exons 5, 6, and 9 of *CYP4V2* in chromosome 4 (Figure 2). Multiplex PCR was performed to amplify five fragments simultaneously according to the manufacturer's instructions (QIAGEN, Hilden, Germany). The genotype of rs397722245 was determined with PCR-based sequencing in the patients and the healthy subjects. Primers for amplification (Table 2) were designed by Primer3. The SNaPshot extension reaction used primers that each consisted of a complementary sequence

(18–20 nucleotides long) with the 3′ end next to the polymorphism site and a poly (GACT), which ensured the spatial resolution of the extension products during capillary electrophoresis. The extension reaction was performed according to the instructions included with the SNaPshot kit (Applied Biosystems). Briefly, the reaction mixture contained 5 µl of SNaPshot ready reaction mix, 1 µM of extension primer for each SNP, and 3 µl of purified multiplex PCR products. The program consisted of 25 cycles at 96 °C for 10 s, 50 °C for 5 s, and 60 °C for 30 s. The extension fragments were incubated with 1 U of shrimp alkaline phosphatase (SAP) at 37 °C for 60 m. The purified products were mixed with HiD formamide and the GeneScan-120 LIZ size standard, followed by capillary electrophoresis on an ABI PRISM 310 Genetic Analyzer (Applied Biosystems, Foster City, CA). Raw data were analyzed with GeneMapper 3.0.

Haplotypes were established according to the genotypes of the six SNPs in the patients, the healthy controls, and patients' relatives. Ambiguous haplotypes in haplotype determination were predicted with the PHASE program [30].

Statistical analysis: The age of disease onset was defined as the age at which symptoms were first noted. The Snellen visual acuity figures were converted into the logarithm of the minimum angle of resolution (logMAR) decimal values for statistical analysis. Values of 0, 1.0, and 2.0 in logMAR are equal to 1.0, 0.1, and counting fingers, respectively, in the Snellen visual acuity test [31]. The chi-square test was used to compare the haplotype distribution between the

Figure 1. Fundus appearance of patients with BCD in stages 1. Stage 1-**A**–**C**; patient 028094), Stage 2-**D**–**F**; patient 028130), and Stage 3-**G**–**I**; patient 028092). **A**: Crystalline deposits in the posterior pole are shown in the color image. **B**: Autofluorescence (AF) was normal in the posterior pole as shown in the fundus autofluorescence (FAF) image. **C**: The RPE layer and the inner retina are normal on spectral domain optical coherence tomography (SD-OCT). **D**: Discoloration and crystalline deposits in the color image extend beyond the posterior pole. **E**: Areas of hypofluorescence and hyperfluorescence are seen beyond the posterior. **F**: Drusen-like deposits and extensive loss of the outer retina are noted. Outer retinal tubulation (the red triangle) is present. **G**: Diffuse atrophy of the RPE and choroidal sclerosis are obvious. The number of crystalline deposits is fewer than in stage 2. Pigment deposits are seen. **H**: The AF in the posterior pole is almost absent. **I**: Diffuse loss of the ellipsoid zone, the interdigitation zone, and the RPE is shown in both eyes of the patient.

TABLE 1. PRIMERS INFORMATION FOR THE REAL–TIME QUANTITATIVE POLYMERASE CHAIN REACTION (PCR).

Gene	Forward sequence (5'-3')	Reverse sequence (5'-3')	Products(bp)	Tm (°C)
CYP4V2 Exon1	GTCTGGTCCTGAGCCTGC	AGGGCAGGGGTTTGGAAATA	378	60
CYP4V2 Exon2	ACTGGTCACAACTTTCTCATCT	TTTGTGCTGAAATGGCTGAAA	275	58
CYP4V2 Exon3	GGACTGAAAATGAACGACGGA	TCCAGCCTTTCTCCTCCTTT	359	60
CYP4V2 Exon4	TCTCTTTCTCTCTCTCTCTCTGT	AGAAAACAGATCGATGAGACTCAC	273	58
CYP4V2 Exon5	CCGCTGCAAAATAAACACGAG	CCTTTACTGCTTAAACACATGCT	300	58
CYP4V2 Exon6	CCCACGATTGCCTTCATCAA	CCACAATTGTAAAAGTCAGGGAC	250	60
CYP4V2 Exon8	CAGTGCAGTCATCAAATCCAGA	GCCTTCCTGCTCATTACACTG	300	58
CYP4V2 Exon9 and Exon10	CGTCCCGCTACAGTAGAAGA	CTCGGATCTCTGTGCAATGC	284	58
CYP4V2 Exon11	CAGGACCTCTTGTTTCTCACA	GCGTTCATCTGCATTTCTCCT	239	60
GAPDH	AGAAGACTGTGGATGGCCC	TCAGTGTAGCCCAGGATGC	280	60

patients and the controls. We classified the patients into three groups: patients with c.802–8_810del17insGC in the homozygous state (n=54), patients with c.802–8_810del17insGC in the heterozygous state (n=50), and patients with non-c.802–8_810del17insGC mutations (n=21). The standard deviation (SD) of the mean onset age was calculated. Analysis of variance (ANOVA) was used to compare the difference in the age of onset between patients with homozygous c.802–8_810del17insGC mutations, compound heterozygous c.802–8_810del17insGC mutations, and non-c.802–8_810del17insGC mutations. All statistical analyses were performed using SPSS version 22 software (IBM Corp., Armonk, NY). The statistical significance level adopted was 5%.

RESULTS

Mutations in CYP4V2: We identified biallelic mutations in *CYP4V2* with direct sequencing in 125 (97.7%) patients, one mutant allele in two (1.5%) patients, and no mutant allele in one (0.8%) patient. We identified 28 disease-causing variants of *CYP4V2* in the cohort patients (Appendix 1), which included 14 missense (50%), five nonsense (17.9%), five splicing defects (17.9%), three small insertion or deletion (10.7%) mutations, and a large deletion mutation (3.5%). Of these 28 mutations, the most common mutation was c.802–8_810del17insGC, with an allele frequency of 62.8%, followed by p.H331P (8.7%), c.1091–2A>G (7.5%), and p.F73L (3.1%) mutations. The remaining 24 mutations in *CYP4V2* accounted for only 17.9% of all mutant alleles. In total, 54 (43%) patients were homozygous for the c.802–8_810del17insGC mutation, while 50 (40%) patients were compound heterozygous. Only 21 (17%) patients were found

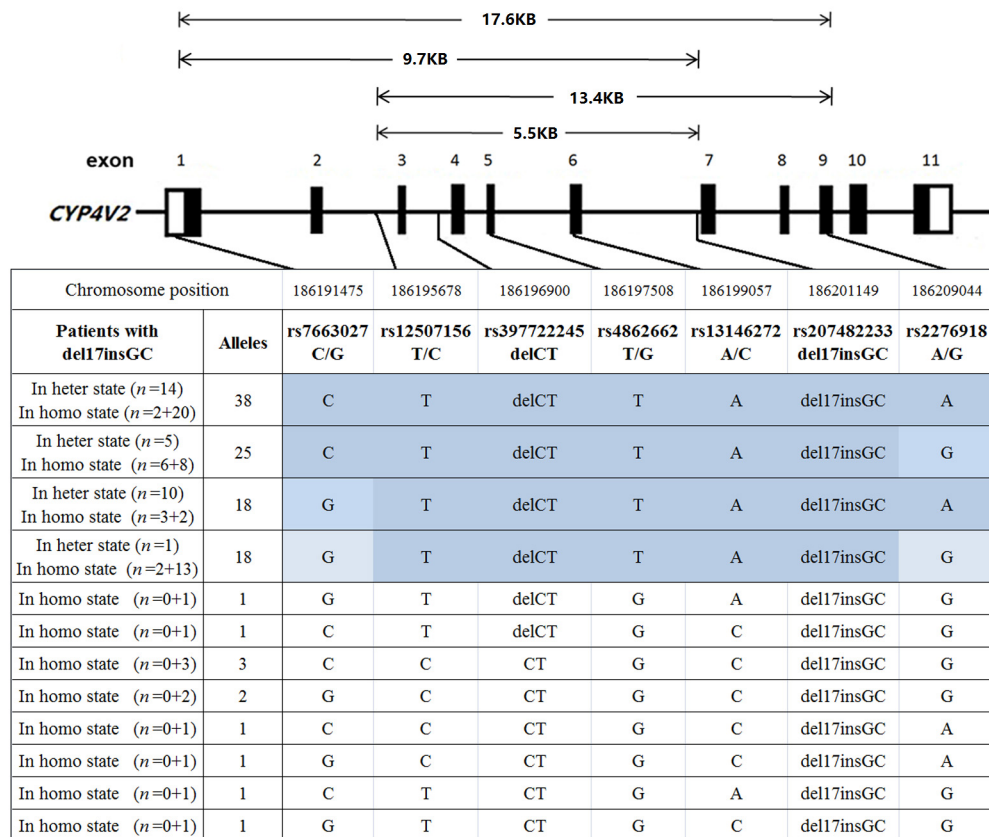| Chromosome position		186191475	186195678	186196900	186197508	186199057	186201149	186209044
Patients with del17insGC	**Alleles**	rs7663027 C/G	rs12507156 T/C	rs397722245 delCT	rs4862662 T/G	rs13146272 A/C	rs207482233 del17insGC	rs2276918 A/G
In heter state (*n*=14) In homo state (*n*=2+20)	38	C	T	delCT	T	A	del17insGC	A
In heter state (*n*=5) In homo state (*n*=6+8)	25	C	T	delCT	T	A	del17insGC	G
In heter state (*n*=10) In homo state (*n*=3+2)	18	G	T	delCT	T	A	del17insGC	A
In heter state (*n*=1) In homo state (*n*=2+13)	18	G	T	delCT	T	A	del17insGC	G
In homo state (*n*=0+1)	1	G	T	delCT	G	A	del17insGC	G
In homo state (*n*=0+1)	1	C	T	delCT	G	C	del17insGC	G
In homo state (*n*=0+3)	3	C	C	CT	G	C	del17insGC	G
In homo state (*n*=0+2)	2	G	C	CT	G	C	del17insGC	G
In homo state (*n*=0+1)	1	C	C	CT	G	C	del17insGC	A
In homo state (*n*=0+1)	1	G	C	CT	G	C	del17insGC	A
In homo state (*n*=0+1)	1	C	T	CT	G	A	del17insGC	G
In homo state (*n*=0+1)	1	G	T	CT	G	C	del17insGC	G

Figure 2. Schematic diagram shows the position of seven single SNPs in *CYP4V2* and haplotypes of 70 patients with the c.802–8_810del17insGC mutation (40 patients in the homozygous state and 30 patients in the heterozygous state). The ancient haplotype is shaded dark blue. Alleles showing recombination from the ancient haplotype are shaded light blue or gray. Alleles beyond the recombination events and not included in the ancient haplotype are not shaded. The number of patients with c.802–8_810del17insGC in the homozygous state (n=homozygous haplotype + heterozygous haplotype).

TABLE 2. PRIMERS INFORMATION FOR AMPLIFICATION AND SNAPSHOT EXTENSION REACTION OF 7 SNPS.

SNP	Primer sequence for PCR (5'-3')	Primer sequence for extension reaction (5'-3')
rs7663027	Forward: GTAGAGCAACCTCGCAGCAC Reverse: GCGTAGTGATTGCACTGGAG	GACTGACTTCCGACGCCCCTGACCCCGCATCC
rs12507156	Forward: TGCTTTCAGACCACAGCAAC Reverse: GCATTCAGTCTTGGGGACTC	GACTGACTGACTGACTCATCTCCCCACATGTGCCCACC
rs4862662	Forward: AGGAAGAACAGGAACAGGGAGTAG Reverse: CAACGCAGAAATTGTTAGCAATAA	GACTGACTGACTGACTGACTGACTTAACGTGCGTGAATTGAATG
rs13146272	Forward: GCTTCATGGGATGCGTAATAGC Reverse: GAAATGAACGGTGGGGATGGT	GACTGACTGACTGACTGACTGACTGACTATGGGAACACAAAAAG AGCCTT
rs2276918	Forward: ATGCCATGCCTTGATCCACCTGT Reverse: TGGGCAATGTCACATCACATCTCA	GACTGACTGACTGACTGACTGACTGACTGACTAAGGGGAGA GGGAAACTTTCT
rs397722245	Forward: TGAGAACCTGTAGATGAAGCTGT Reverse: TCGATGAGACTCACCACAGA	
rs207482233	Forward: CCCCAAAATATTAATGAGGCTTT Reverse: TTGTTTAATGATATCTGAACCTAACAA	

to be harboring non-c.802–8_810del17insGC mutations. Of the 54 patients with the c.802–8_810del17insGC mutation in the homozygous state, only seven (13%) patients were from a consanguineous marriage. Cosegregation analysis performed in 14 families showed that their parents each carried a wild-type and a heterozygous mutant allele, with the exception of the pedigree of patient 0191002, whose mother also harbored

this mutation in its homozygous state (Figure 3). In the following clinical examination, the patient's mother was diagnosed with BCD. We screened the c.802–8_810del17insGC mutation in 421 healthy Chinese controls and detected three heterozygous mutations, a 0.36% frequency.

Of the 28 mutations, eight were first identified in the present study. The novel mutations include four missense
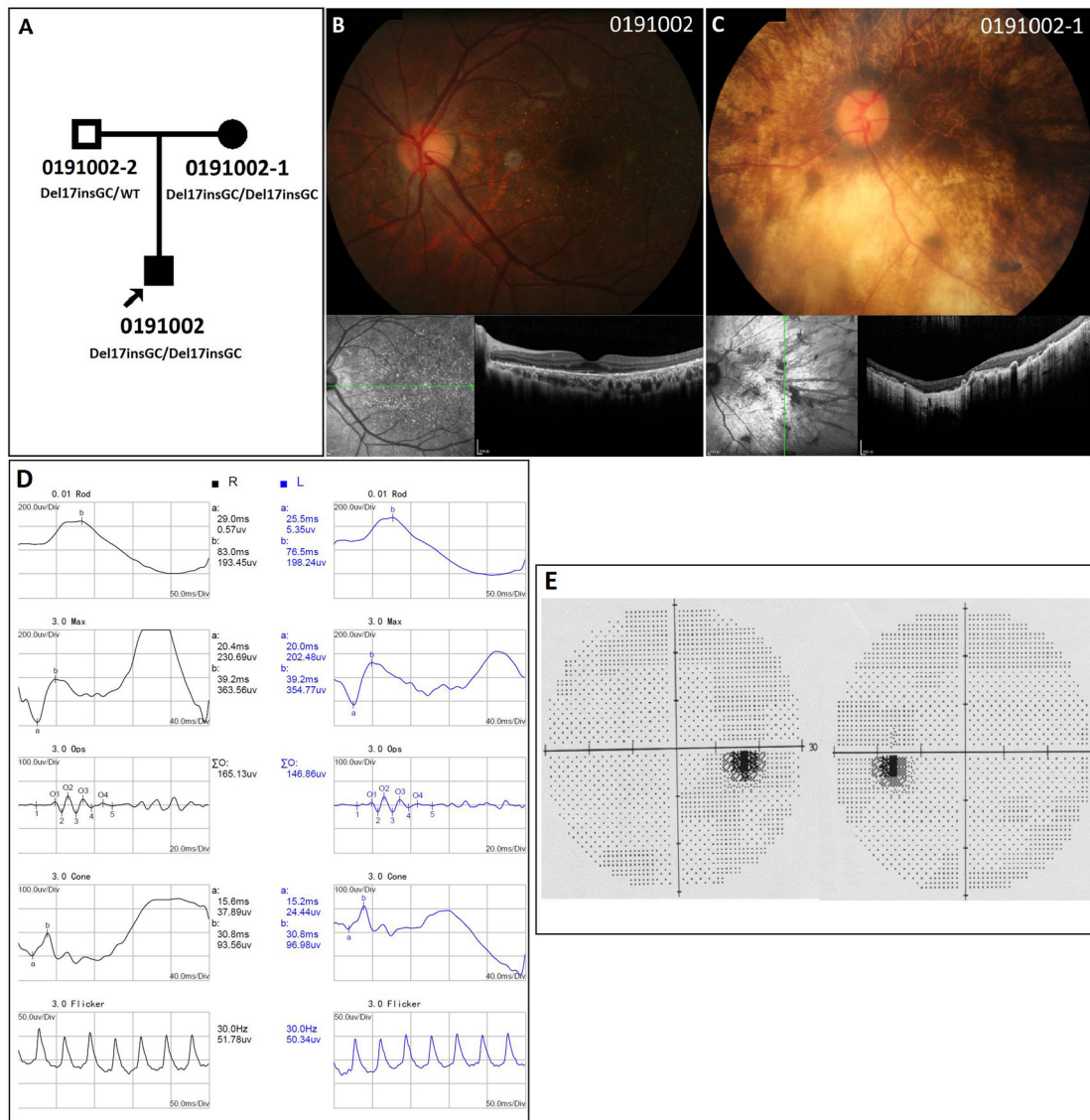
Figure 3. Pedigree, fundus appearances, macular SD-OCT, ERG, and visual field images of patient 0191002. **A**: Pedigree of family 0191002 and segregation analysis of the homozygous mutation c.802–8_810del17insGC/ c.802–8_810del17insGC. **B**: Fundus photograph of the left eye of patient 0191002 shows typical crystalline deposits in the macular region. The spectral domain optical coherence tomography (SD-OCT) photo shows hyper-reflective material deposits in the RPE layer and RPE detachment. **C**: The fundus photograph of the left eye of the mother of patient 0,191,002 shows pigment deposits and choroidal sclerosi in the posterior pole. The SD-OCT image shows disruption of the structure of the outer retina and atrophy of the choroidal vessels. **D**: The amplitude of 30 Hz flicker reaction in the electroretinography (ERG) of patient 0191002 was mildly reduced. **E**: Central visual field of patient 0191002 measured using a Humphrey field analyzer with a SITA 30–2 program is within normal limits.

mutations, one nonsense mutations, two splicing mutations, and one large deletion mutation. Four missense mutations (p.C406R, p.C467Y, p.G503E, and p.L426F) were predicted to be disease-causing by at least two in silico analysis programs and were classified as likely pathogenic according to the ACMG guidelines. Two novel splicing mutations, c.801+5G>A and c.802−9A>G, were predicted to cause a normal splice donor loss and create a new splice acceptor, respectively. Genomic quantitative PCR analysis revealed a heterozygous large deletion encompassing exon 8 of *CYP4V2* in patient 028,147. Long-range PCR was performed but failed to find the breakpoints. None of the eight novel mutations was observed in a panel of 200 normal subject alleles, and most of the mutations were not found in any public databases, including the European Voluntary Service (EVS), 1000 Genomes, the Exome Aggregation Consortium (ExAC), and the Genome Aggregation Database (gnomAD; Appendix 1).

In addition, two novel missense variants, p. R85H and p. M123R, were predicted to be benign by most of the in silico programs, but the GERP++ score for these two variants was 5.55 and 5.58, respectively, implying highly conserved sites of R85 and M123. Although the variants were not described in any public databases and not detected in 100 healthy controls, the variants were defined as variants of uncertain significance in the present study.

Haplotype analysis: Intragenic SNP haplotype analysis revealed four common haplotypes in patients with the c.802−8_810del17insGC mutation (Figure 2). Individual alleles of the seven SNPs composing the haplotypes were highly conserved among the patients: rs7663027 (63% C), rs12507156 (94% T), rs397722245 (93% delCT), rs4862662 (90% T), rs13146272 (92% A), rs207482233 (100% the c.802−8_810del17insGC indel), and rs2276918 (53% A). In the controls, the allele frequencies for these seven SNPs were 43% of C, 35% of T, 31% of delCT, 31% of T, 38% of A, 0% of the c.802−8_810del17insGC indel, and 67% of A, respectively. The most common haplotype CT(delCT)TA(Indel)A, spanning 17.6 kb from 5′-UTR to exon 9 of *CYP4V2*, was harbored by 34.5% (38/110) of the c.802−8_810del17insGC mutant alleles. The haplotypes CT(delCT)TA(Indel)G, GT(delCT)TA(Indel)A, and GT(delCT)TA(Indel)G, were observed in 22.7% (25/110), 16.4% (18/110), and 16.4% (18/110), respectively, of the mutant c.802−8_810del17insGC alleles. All four haplotypes shared a 5.5 kb chromosome region spanning IVS2 to IVS6 of *CYP4V2*. The four haplotypes were not observed in the controls. The partial haplotypes, CT(delCT)TAA, CT(delCT)TAG, GT(delCT)TAA, and GT(delCT)TAG, were observed in 11.8% (22/186), 10.8% (20/186), 1.6% (3/186), and 6.5% (12/186), respectively, of the normal alleles in the controls. The difference between the four partial haplotype frequencies in the normal alleles and the mutant alleles was statistically significant (p<0.01).

Clinical profiles and genotype-phenotype correlation: One hundred and twenty-five unrelated patients with BCD were found to harbor two disease-causing mutations in *CYP4V2*, and cosegregation analyses were performed in 42 (34%) patients. (See Appendix 2 for a summary of the clinical phenotype of the patients with BCD.) The patients with mutations in *CYP4V2* in this cohort showed phenotypic variability. Their age of onset of BCD ranged from 6.0 to 72 years (mean 28.4±9.80); the logarithm of the minimum angle of resolution (logMAR) BCVA ranged from 0 to 5. As expected, the patients in stage 1 had mild visual defects, while the patients in stage 3 usually showed severe visual impairment. The majority of patients first experienced either night blindness or defects in visual acuity. Three patients in stage 1 did not have any symptoms, but routine examination showed abnormal fundus appearances. Fundus examinations revealed that all patients had intraretinal crystalline deposits in their posterior pole with different extents of RPE atrophy or choroidal sclerosis (Figure 1). The patients in stages 1 and 2 revealed more crystal deposits in their fundus than the patients in stage 3 (Figure 1). On the slit-lamp examination, corneal limbal crystals were observed in both eyes of three patients (028059, 028095, and 028164). SD-OCT revealed intraretinal hyper-reflective granules, outer retinal tubulation, drusen-like deposits, and extensive loss of the outer retina in patients in stages 2 and 3 (Figure 1). The patients in stage 1 presented an almost normal FAF while the patients in stages 2 and 3 showed different hypofluorescent regions in the posterior pole or in almost the entire retina (Figure 1). ERG recording of the patients in stage 1 presented an almost normal or slightly decreased cone function (Figure 3D), while ERG examinations of the patients in stage 2 or 3 showed reductions in cone and rod function or extinguished recordings.

The mean age of onset for patients with c.802−8_810del17insGC in the homozygous state, heterozygous state, and those with non-c.802−8_810del17insGC mutations, was 28.5±10.1, 26.6±9.30, and 32.5±10.2 years, respectively. The difference in the mean age of onset between the patients with compound heterozygous c.802−8_810del17insGC mutations and those with non-c.802−8_810del17insGC mutations was statistically significant (p=0.018).

DISCUSSION

This study presents a comprehensive molecular analysis of *CYP4V2* in a large cohort of Chinese patients with BCD. In this study, mutations in *CYP4V2* were detected in 97.7% of patients, which is consistent with the results reported in two previous Chinese studies [12,21]. The higher detection rate is due to the homogeneity of BCD both genetically and clinically [3,12]. Patients with BCD, especially patients in stage 1 or 2, usually had characteristic typical yellow-white crystalline deposits in the fundi, making correct diagnosis of these patients simple. With disease progression, typical yellow-white crystalline deposits in the fundi of patients in stage 3 decrease, and thus, it is difficult to distinguish between this type of patient and patients with other inherited retinal diseases in late stage, such as patients with Stargardt disease (STGD) in stage IV (Figure 4) [32] or patients with choroideremia, whose fundi also show severe RPE and chorioretinal atrophy.

Although we identified 28 disease-causing mutations in this cohort of patients, the three common mutations (c.802–8_810del17insGC, p.H331P, and c.1091–2A>G) accounted for almost 80% of all mutant alleles. This is consistent with
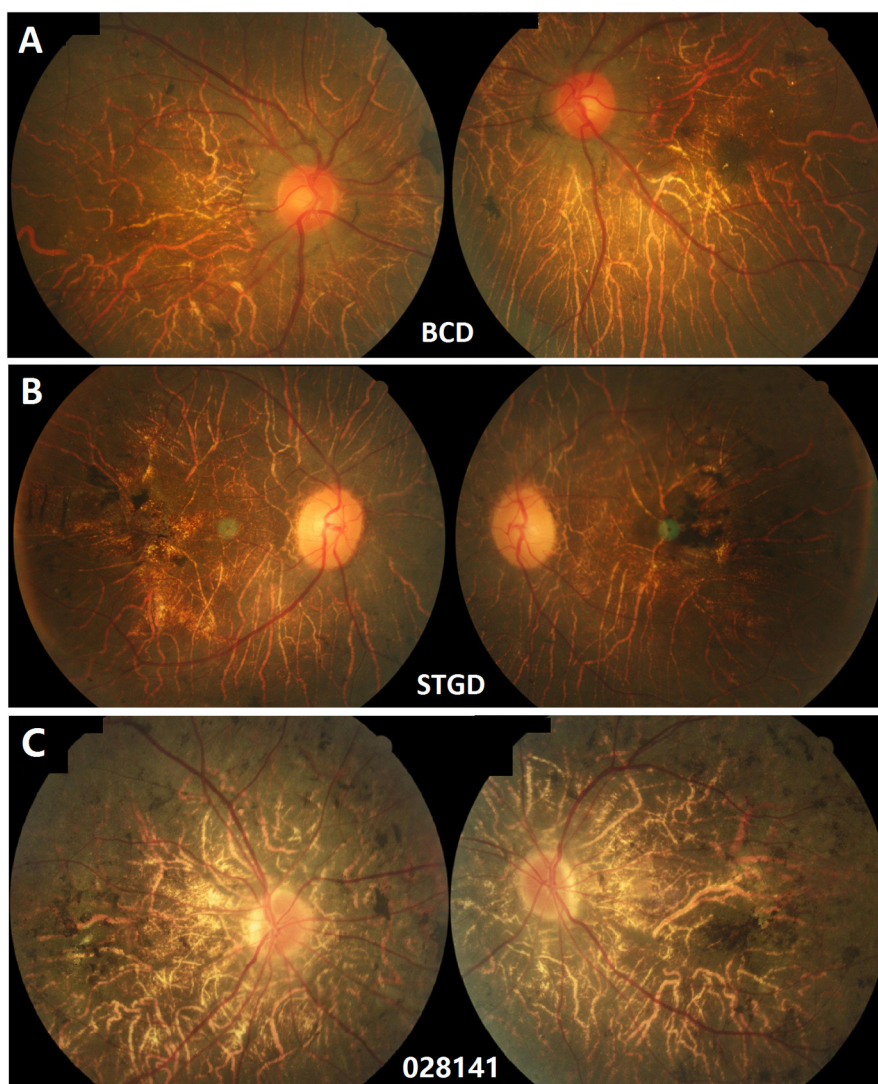

Figure 4. Fundus images of three patients with BCD or STGD. **A**: Fundus images of patient 019,976 in stage 3, carrying the mutations in *CYP4V2* c.802–8_810del17insGC/p.L426F show a few crystal deposits, RPE atrophy, choroidal sclerosis, and pigment deposits. **B**: Fundus images of patient 019491 with Stargardt disease (STGD) in stage 4, carrying mutations in *ABCA4* c.5196+1G>A/c.4773+1G>T [32], display a similar fundus appearance except the crystal deposits. **C**: Patient 028,141 without a mutation in *CYP4V2* in the present study shows RPE atrophy, choroidal sclerosis, and pigment deposits.

several previous observations in Chinese patients with BCD [3,12,19,21,22]. These three common mutations have been reported only in East Asian patients with BCD [3,7-12,19,21,22]. In contrast, two common mutations, p.M66R [20] and p.I111T [16,17,23], found in patients of South Asian and European ancestry with BCD were not observed in the present study cohort. The results further confirmed that the mutation spectrum is ethnically specific. In the present study, we first identified a novel heterozygous large deletion spanning exon 8 of *CYP4V2* in a Chinese patient with BCD 028144. Previously, an approximate 4 Mb deletion encompassing the entire *CYP4V2* and several other genes was identified in a patient with BCD from Germany [23]. For patients with only one identified disease-causing mutation, screening of copy number variations (CNVs) of *CYP4V2* should be considered. Two patients, 028116 and 019122, were found to be carrying a heterozygous c.802−8_810del17insGC mutation and an uncertain variant p.R85H or p.M123R. No CNVs were identified via quantitative PCR analysis. As we did not perform a cosegregation analysis for the variants in the two patients, we describe them as patients with one diseasing-causing mutation identified. In the present study, only patient 028,141 was found to not be carrying any mutations in *CYP4V2*. We revaluated this patient's color fundi photographs and found no typical yellow-white crystalline deposits in the fundi (Figure 4). We considered the patient might be misdiagnosed; next-generation sequencing, screening for other inherited retinal degeneration (IRD) genes, will be performed on this patient in the future.

In two previous studies, the most common mutation, c.802−8_810del17insGC, was shown to be an ancient founder mutation, associated with an 8.5 kb haplotype from IVS3 to IVS8 [7] and a 6.7 kb haplotype from IVS1 to IVS6 of *CYP4V2* [10]. In a recent study, Jiao and colleagues found that an ancient 17.6 kb haplotype CAAT(delCT)TA(indel)TCA was associated with the c.802−8_810del17insGC mutation in 38% (6/16) of Chinese and 36% (5/14) of Japanese mutant alleles [25]. In the present study, we found four different common haplotypes in 90% (99/110) of the mutant alleles. These values are consistent with previous observations [7,10,25]. The most common haplotype CT(delCT)TA(Indel) A in the present study covered almost the same chromosome region described by Jiao and colleagues [25]. According to their mutation age study [25], this haplotype was a common ancient risk haplotype for Chinese, Japanese, and Korean populations, while the other three haplotypes in the present study might be generated from the ancient founder haplotype by one or two recombination events.

Although 83% of the patients in this study carried the c.802−8_810del17insGC mutation, we did not find a distinct genotype-phenotype correlation; however, the patients with c.802−8_810del17insGC showed a relatively early age of disease onset. In the present study, crystals in the limbus cornea were observed only in three unrelated patients (2.4%), which is statistically significantly lower than the rate of 42.4% reported in a previous Chinese study [21] but is consistent with several previous observations in Chinese patients with BCD [7,12,19]. One possibility for this low rate is that the number of patients with limbal deposits may be underestimated, as the limbal deposits are usually smaller than 15 μm, and some can be detected clearly only with specular microscopy [10,33]. We were not certain whether the limbal deposits would decrease with disease progression as the crystal deposits change in terms of occurrence in the retina; if so, the low rate might be related to the high percentage of patients in stage 3 (48%). In the present cohort, some patients did not undergo SD-OCT, FAF, or ERG examination, which was a limitation of the present study. The other limitation was that fewer than half of the patients underwent cosegregation analysis.

In conclusion, the results expand the spectrum of mutations in *CYP4V2* and further verify that the c.802−8_810del17insGC mutation is an ancient founder mutation in a large cohort of Chinese patients. The patient with c.802−8_810del17insGC had an early age of onset.

APPENDIX 1. *CYP4V2* VARIANTS IDENTIFIED IN THIS STUDY AND ANALYSIS OF THE VARIANTS BY PREDICTIVE PROGRAMS.

To access the data, click or select the words "Appendix 1."

APPENDIX 2. THE CLINICAL FEATURE AND THE MUTATION SCREENING RESULTS OF THE *CYP4V2* OF THE BCD PATIENTS IN THIS STUDY.

To access the data, click or select the words "Appendix 2."

ACKNOWLEDGMENTS

REFERENCES

1. Kaiser-Kupfer MI, Chan CC, Markello TC, Crawford MA, Caruso RC, Csaky KG, Guo J, Gahl WA. Clinical biochemical and pathologic correlations in Bietti's crystalline dystrophy. Am J Ophthalmol 1994; 118:569-82. [PMID: 7977570].

2.   Hu DN. Ophthalmic genetics in China. Ophthalmic Paediatr Genet 2009; 2:39-45. .

3.   Li A, Jiao X, Munier FL, Schorderet DF, Yao W, Iwata F, Hayakawa M, Kanai A, Shy Chen M, Alan Lewis R, Heckenlively J, Weleber RG, Traboulsi EI, Zhang Q, Xiao X, Kaiser-Kupfer M, Sergeev YV, Hejtmancik JF. Bietti crystalline corneoretinal dystrophy is caused by mutations in the novel gene CYP4V2. Am J Hum Genet 2004; 74:817-26. [PMID: 15042513].

4.   Miyata M, Hata M, Ooto S, Ogino K, Gotoh N, Morooka S, Hasegawa T, Hirashima T, Sugahara M, Kuroda Y, Yamashiro K, Yoshimura N. Choroidal and retinal atrophy of Bietti crystalline dystrophy patients with CYP4V2 mutations compared to retinitis pigmentosa patients with EYS mutations. Retina 2017; 37:1193-202. [PMID: 27658286].

5.   Miyata M, Ooto S, Ogino K, Gotoh N, Morooka S, Makiyama Y, Hasegawa T, Sugahara M. Hata 2, Yamashiro K, Yoshimura N. Evaluation of Photoreceptors in Bietti Crystalline Dystrophy with CYP4V2 Mutations Using Adaptive Optics Scanning Laser Ophthalmoscopy. Am J Ophthalmol 2016; 161:196-205. [PMID: 26521715].

6.   Chung JK, Shin JH, Jeon BR, Ki CS, Park TK. Optical coherence tomographic findings of crystal deposits in the lens and cornea in Bietti crystalline corneoretinopathy associated with mutation in the CYP4V2. Jpn J Ophthalmol 2013; 57:447-50. [PMID: 23793346].

7.   Lee KY, Koh AH, Aung T, Yong VH, Yeung K, Ang CL, Vithana EN. Characterization of Bietti crystalline dystrophy patients with CYP4V2 mutations. Invest Ophthalmol Vis Sci 2005; 46:3812-6. [PMID: 16186368].

8.   Shan M, Dong B, Zhao X, Wang J, Li G, Yang Y, Li Y. Novel mutations in the CYP4V2 associated with Bietti crystalline corneoretinal dystrophy. Mol Vis 2005; 11:738-43. [PMID: 16179904].

9.   Gekka T, Hayashi T, Takeuchi T, Goto-Omoto S, Kitahara K. CYP4V2 mutations in two Japanese patients with Bietti's crystalline dystrophy. Ophthalmic Res 2005; 37:262-9. [PMID: 16088246].

10. Lin J, Nishiguchi KM, Nakamura M, Dryja TP, Berson EL, Miyake Y. Recessive mutations in the CYP4V2 in East Asian and Middle Eastern patients with Bietti crystalline corneoretinal dystrophy. J Med Genet 2005; 42:e38-[PMID: 15937078].

11. Lai TY, Ng TK, Tam PO, Yam GH, Ngai JW, Chan WM, Liu DT, Lam DS, Pang CP. Genotype phenotype analysis of Bietti's crystalline dystrophy in patients with CYP4V2 mutations. Invest Ophthalmol Vis Sci 2007; 48:5212-20. [PMID: 17962476].

12. Xiao X, Mai G, Li S, Guo X, Zhang Q. Identification of CYP4V2 mutation in 21 families and overview of mutation spectrum in Bietti crystalline corneoretinal dystrophy. Biochem Biophys Res Commun 2011; 409:181-6. [PMID: 21565171].

13. Nakano M, Kelly EJ, Wiek C, Hanenberg H, Rettie AE. CYP4V2 in Bietti's crystalline dystrophy: ocular localization,

metabolism of ω-3-polyunsaturated fatty acids, and functional deficit of the p.H331P variant. Mol Pharmacol 2012; 82:679-86. [PMID: 22772592].

14. Lee J, Jiao X, Hejtmancik JF, Kaiser-Kupfer M, Gahl WA, Markello TC, Guo J, Chader GJ. The metabolism of fatty acids in human Bietti crystalline dystrophy. Invest Ophthalmol Vis Sci 2001; 42:1707-14. [PMID: 11431432].

15. Lai TY, Chu KO, Chan KP, Ng TK, Yam GH, Lam DS, Pang CP. Alterations in serum fatty acid concentrations and desaturase activities in Bietti crystalline dystrophy unaffected by CYP4V2 genotypes. Invest Ophthalmol Vis Sci 2010; 51:1092-7. [PMID: 19797200].

16. Haddad NM, Waked N, Bejjani R, Khoueir Z, Chouery E, Corbani S, Mégarbané A. Clinical and molecular findings in three Lebanese families with Bietti crystalline dystrophy: report on a novel mutation. Mol Vis 2012; 18:1182-8. [PMID: 22605929].

17. Rossi S, Testa F, Li A, Yaylacioğlu F, Gesualdo C, Hejtmancik JF, Simonelli F. Clinical and genetic features in Italian Bietti crystalline dystrophy patients. Br J Ophthalmol 2013; 97:174-9. [PMID: 23221965].

18. García-García GP, López-Garrido MP, Martínez-Rubio M, Moya-Moya MA, Belmonte-Martínez J, Escribano J. Genotype-phenotype analysis of Bietti crystalline dystrophy in a family with the CYP4V2 Ile111Thr mutation. Cornea 2013; 32:1002-8. [PMID: 23538635].

19. Yin H, Jin C, Fang X, Miao Q, Zhao Y, Chen Z, Su Z, Ye P, Wang Y, Yin J. Molecular analysis and phenotypic study in 14 Chinese families with Bietti crystalline dystrophy. PLoS One 2014; 9:e94960-[PMID: 24739949].

20. Halford S, Liew G, Mackay DS, Sergouniotis PI, Holt R, Broadgate S, Volpi EV, Ocaka L, Robson AG, Holder GE, Moore AT, Michaelides M, Webster AR. Detailed phenotypic and genotypic characterization of Bietti crystalline dystrophy. Ophthalmology 2014; 121:1174-84. [PMID: 24480711].

21. Meng XH, Guo H, Xu HW, Li QY, Jin X, Bai Y, Li SY, Yin ZQ. Identification of novel CYP4V2 mutations in 92 Chinese families with Bietti's crystalline corneoretinal dystrophy. Mol Vis 2014; 20:1806-14. [PMID: 25593508].

22. Tian R, Wang SR, Wang J, Chen YX. Novel CYP4V2 mutations associated with Bietti crystalline corneoretinal dystrophy in Chinese patients. Int J Ophthalmol 2015; 8:465-9. [PMID: 26085992].

23. Astuti GD, Sun V, Bauwens M, Zobor D, Leroy BP, Omar A, Jurklies B, Lopez I, Ren H, Yazar V, Hamel C, Kellner U, Wissinger B, Kohl S, De Baere E, Collin RW, Koenekoop RK. Novel insights into the molecular pathogenesis of CYP4V2-associated Bietti's retinal dystrophy. Mol Genet Genomic Med 2015; 3:14-29. [PMID: 25629076].

24. Yin X, Yang L, Chen N, Cui H, Zhao L, Feng L, Li A, Zhang H, Ma Z, Li G. Identification of CYP4V2 mutation in 36 Chinese families with Bietti crystalline corneoretinal dystrophy. Exp Eye Res 2016; 146:154-62. [PMID: 26971461].

25. Jiao X, Li A, Jin ZB, Wang X, Iannaccone A, Traboulsi EI, Gorin MB, Simonelli F, Hejtmancik JF. Identification and population history of CYP4V2 mutations in patients with Bietti crystalline corneoretinal dystrophy. Eur J Human Genetics: EJHG 2017; 25:461-71. [PMID: 28051075].

26. Li Q, Li Y, Zhang X, Xu Z, Zhu X, Ma K, She H, Peng X. Utilization of fundus autofluorescence, spectral domain optical coherence tomography, and enhanced depth imaging in the characterization of Bietti crystalline dystrophy in different stages. Retina 2015; 35:2074-84. [PMID: 25978730].

27. Yuzawa M, Mae Y, Matsui M. Bietti's crystalline retinopathy. Ophthalmic Paediatr Genet 1986; 7:9-20. [PMID: 3703493].

28. Richards S, Aziz N, Bale S, Bick D, Das S, Gastier-Foster J, Grody WW, Hegde M, Lyon E, Spector E, Voelkerding K, Rehm HL. ACMG Laboratory Quality Assurance Committee. Standards and guidelines for the interpretation of sequence variants: a joint consensus recommendation of the American College of Medical Genetics and Genomics and the Association for Molecular Pathology. Genet Med 2015; 17:405-24. [PMID: 25741868].

29. Livak KJ, Schmittgen TD. Analysis of relative gene expression data using real-time quantitative PCR and the 2-DDCT method. Methods 2001; 25:402-8. [PMID: 11846609].

30. Stephens M, Smith NJ, Donnelly P. A new statistical method for haplotype reconstruction from population data. Am J Hum Genet 2001; 68:978-89. [PMID: 11254454].

31. Holladay JT. Proper method for calculating average visual acuity. J Refract Surg 1997; 13:388-91. [PMID: 9268940].

32. Jiang F, Pan Z, Xu K, Tian L, Xie Y, Zhang X, Chen J, Dong B, Li Y. Screening of ABCA4 gene in a Chinese cohort with Stargardt disease or Cone-rod dystrophy with a report on 85 novel mutations. Invest Ophthalmol Vis Sci 2016; 57:145-52. [PMID: 26780318].

33. Mataftsi A, Zografos L, Millá E, Secrétan M, Munier FL. Bietti's crystalline corneoretinal dystrophy: a cross-sectional study. Retina 2004; 24:416-26. [PMID: 15187665].